



## Chronic home radon exposure impacts the development of oscillatory dynamics serving visuospatial attention

Rachel A. Bonney<sup>a,b,1</sup> , Sarah L. Greenwood<sup>a,b</sup>, Danielle Thompson<sup>a,b,2</sup>,  
 Monica N. Clarke-Smith<sup>a,b</sup>, Saige C. Rasmussen<sup>a,b</sup>, Grace E. Parolek<sup>a,b</sup>,  
 OgheneTejiri V. Smith<sup>a,b,3</sup>, Haley R. Pulliam<sup>a,b,4</sup>, Brittany K. Taylor<sup>a,b,c,\*</sup> 

<sup>a</sup> Institute for Human Neuroscience, Boys Town National Research Hospital, Boys Town, NE, USA

<sup>b</sup> Center for Pediatric Brain Health, Boys Town National Research Hospital, Boys Town, NE, USA

<sup>c</sup> Department of Pharmacology and Neuroscience, Creighton University, Omaha, NE, USA

### ARTICLE INFO

#### Keywords:

Environmental exposure  
 Magnetoencephalography (MEG)  
 Neurodevelopment  
 Visuospatial attention  
 Ventral attention network (VAN)  
 Attention deficit hyperactivity disorder (ADHD)

### ABSTRACT

Radon is a naturally occurring gas that can accumulate to hazardous levels in homes. While previous work has shown that environmental toxicants negatively impact neurodevelopment, little is understood about how radon may affect critical cognitive functions like visuospatial attention, which is subserved by multispectral neural oscillatory dynamics across the developmentally-sensitive attention networks. This study explored the effects of chronic home radon exposure on the developmental trajectories of oscillatory dynamics serving visuospatial attention in youths. We recruited 118 youths aged 8-to-15 years-old to complete a visuospatial attention task during magnetoencephalography. Families completed a home radon test, and inattention and hyperactivity symptoms were measured using a self-report questionnaire. We found functionally relevant radon-related aberrations to beta dynamics within the left inferior frontal (IFG) and superior temporal gyrus. In both regions, children with higher radon exposure exhibited stronger beta responses as a function of age, which predicted slower reaction times. Age-related strengthening of beta responses in the IFG was also correlated with lesser attentional symptomatology. These results suggest aberrant developmental trajectories of neural processing as a function of increasing radon exposure in critical attention regions, which may indicate compensatory activity to sustain performance and improve attentional stability despite chronic environmental insult.

### 1. Introduction

Visuospatial processing is vital to everyday function, as we must be able to identify and locate stimuli, interpret spatial relationships, and organize visual information to ultimately facilitate appropriate interaction with the environment. Visual information travels from the retina through the thalamus to bilateral occipital cortices, which relay the information to higher-order frontoparietal networks that provide feedback to guide the allocation of visuospatial attention (Bisley, 2011; Trés and Brucki, 2014). Classical visuospatial attention networks include the dorsal attention network (DAN) and the ventral attention network (VAN). The DAN is comprised of occipital, parietal, and dorsolateral

prefrontal areas and is responsible for spatial orienting and implementing goal-directed action. Alternatively, the VAN is localized to occipital and temporal areas, and is involved in object identification and the facilitation of stimulus-driven responses (Corbetta and Shulman, 2002; Tosoni et al., 2023).

Deficits in visuospatial functioning have been associated with neurodevelopmental disorders including developmental coordination disorder, specific learning disorder, autism spectrum disorder, attention deficit hyperactivity disorder (ADHD), and broad reading and academic challenges (Cardillo et al., 2020; Franceschini et al., 2022; Pisella et al., 2021). Thus, the timely and efficient development of attentional processing faculties is of great interest and importance. The neural

\* Correspondence to: Boys Town National Research Hospital, Institute for Human Neuroscience, 14090 Mother Teresa Ln, Boys Town, NE 68010, USA.

E-mail address: [Brittany.Taylor@boystown.org](mailto:Brittany.Taylor@boystown.org) (B.K. Taylor).

<sup>1</sup> Neuroscience Center, Brigham Young University, Provo, UT, USA

<sup>2</sup> School of Medicine, Medical College of Wisconsin, Milwaukee, WI, USA

<sup>3</sup> Department of Psychology, Temple University, Philadelphia, PA, USA

<sup>4</sup> School of Medicine, Creighton University, Phoenix, AZ, USA

oscillatory dynamics that facilitate processing throughout these complex, interconnected visuospatial networks are multispectral in nature, spanning theta (4–8 Hz), alpha (8–12 Hz), beta (12–30 Hz), and gamma (> 30 Hz) oscillations (Wiesman et al., 2017). These dynamics rapidly mature throughout adolescence, with studies showing developmental changes in alpha, theta, and gamma oscillatory activity that are influenced by age, pubertal hormones, and sex (Fung et al., 2020, 2022; Killanin et al., 2020). Researchers have suggested that changes in oscillatory dynamics during development represent critical network reorganization that ultimately supports the refinement and maturation of functional brain networks (Taylor et al., 2022; Uhlhaas et al., 2009).

The period from late childhood into adolescence has been recently identified as a sensitive period of development for higher-order cognitive networks, including the DAN and VAN (Larsen and Luna, 2018). With heightened plasticity comes greater vulnerability to maladaptive experiences and exposures, including inhaled environmental toxicants. Exposures to inhaled pollutants during childhood have been found to alter brain structure (Beckwith et al., 2020; Cserbik et al., 2020; Smith et al., 2024) and functional network connectivity (Cotter et al., 2023; Kusters et al., 2025). Toxic environmental exposures have also been linked to adverse mental and behavioral health outcomes (Miller et al., 2019; Roberts et al., 2019; Taylor et al., 2024), especially attention deficit hyperactivity disorder (Bernardina Dalla et al., 2022; Min and Min, 2017; Myhre et al., 2018; Newman et al., 2013; Peterson et al., 2015; Thygesen et al., 2020). While an extensive and growing body of literature has characterized the effects of various toxicants on neurocognitive development, the effects of some pervasive toxicants, such as radon gas, have seldom been explored.

Radon is a colorless, odorless, ubiquitous radioactive gas emitted from natural uranium decay in the ground that can accumulate to hazardous levels in homes (Clement et al., 2010; Darby et al., 2005; Grzywa-Celińska et al., 2020; Kang et al., 2019; Sethi et al., 2012). The Environmental Protection Agency (EPA) estimates that 1 in 15 homes in the United States exceed the current action limit of 4.0 pCi/L (148 Bq/m<sup>3</sup>), and further states that even levels below this limit pose risks (United States Environmental Protection Agency, 2016). Despite its known health hazards, public awareness of radon remains low (Novilla et al., 2021; Vogeltanz-Holm and Schwartz, 2018). Radon has historically been linked to lung cancer (Riudavets et al., 2022; Sethi et al., 2012; Vogeltanz-Holm and Schwartz, 2018) and neurodegenerative diseases in adulthood (Gómez-Anca and Barros-Dios, 2020; Zhang et al., 2022). Recent work has explored radon's effects on the developing brain, with chronic exposure in homes linked to increased concentrations of neuroinflammatory biomarkers in children and adolescents (Taylor et al., 2022), lower gray matter volumes (Smith et al., 2024), increased self- and emotion-regulation dysfunction (Taylor et al., 2024), and aberrations in oscillatory dynamics serving attentional reorienting (Pulliam et al., 2024). These findings underscore the need to characterize radon's effects on neural and behavioral changes throughout child cognitive development, especially within critical cognitive brain networks like the DAN and VAN.

The present study investigated the impact of chronic home radon exposure on the developmental trajectories of neural oscillatory dynamics serving visuospatial attention processing in typically-developing children and adolescents. To measure the neural processing underlying visuospatial attention, youths completed a visuospatial processing task while having their functional brain activity recorded during magnetoencephalography (MEG). Home radon test kits were used to measure indoor radon concentrations in the family home. To probe behavioral outcomes, participants' inattention and hyperactivity symptoms were measured using a well-validated questionnaire of children's neuropsychological symptoms and behaviors. We hypothesized that radon exposure would significantly modulate developmental trajectories of neural dynamics serving visuospatial attention in key regions spanning the DAN and VAN. We also expected these aberrations to mediate the effects of radon exposure on behavioral outcomes and attentional

symptoms (i.e., ADHD symptomology).

## 2. Methods and materials

### 2.1. Participants

We studied 118 healthy children aged 8–15 years old ( $M = 12.09 \pm 2.31$  years, 61 males) who were recruited from the local community. All participants were typically developing, without any history of head trauma, neurological or psychiatric disorders, or other disorders affecting brain function. Exclusionary criteria included general MEG/MRI contraindications (e.g., the presence of dental braces, permanent retainers, and/or any type of ferromagnetic non-removable devices), as well as history of head trauma, epilepsy, neurodevelopmental disorders, or other conditions affecting the central nervous system, and current use of substances or medications known to alter brain function. Inclusion and exclusion were confirmed through participant interviews involving the child and parent. After a complete description of the study, written informed consent was obtained from the legally authorized representative of each participant, and participants provided assent. All procedures were approved by the Institutional Review Board (protocol #21-16-XP, approved July 19, 2021).

### 2.2. Radon data collection

Families were provided with a commercial long-term home radon testing kit (<https://www.radon.com/>). The test kit is a standard alpha-track radon detector that is placed in the lowest livable level of the home for 30 days in accordance with instruction provided by the vendor. After the testing period, the kit is placed in a box and sent in for processing at a commercial lab. Our lab and the family each received a copy of the home radon results. In the case that a result exceeded the EPA action limit for mitigation (4 pCi/L), the principal investigator (BKT) called the family to ensure they understood the results and provided additional information on radon safety and local resources. In addition to completing the radon test kit, parents completed a questionnaire probing information about how long the child had lived in the home, the construction of their home, and other details to help characterize home radon exposure. We used the information about how long the child had lived in the home to compute a radon exposure index. Specifically, each child's individual radon exposure index was computed as the natural log of the measured home radon concentration multiplied by the duration that the child had lived in the home (in years), plus one to account for the natural log transform (see Eq. 1 below; (Pulliam et al., 2024; Smith et al., 2024; Taylor et al., 2024, 2022)). This radon exposure index (REI) was used as a measure of cumulative exposure in subsequent analyses exploring the associations between chronic home radon exposure and neural dynamics.

$$\text{Radon exposure index} = \ln([\text{time lived in home}] * [\text{home radon concentration}]) + 1 \quad (1)$$

### 2.3. Inattention/hyperactivity data

Participants' attentionally-relevant symptoms were measured through the age-appropriate self-report of the Behavior Assessment System for Children, 3rd Edition (BASC-3) (Reynolds and Kamphaus, 2015). Children rated the frequency with which each item described their behavior on a 4-point scale (0 = never, 1 = sometimes, 2 = often, 3 = almost always). The Inattention/Hyperactivity subscale, which was the focus of our investigation, is comprised of 13 items for a total possible raw score range of 0–39, with higher scores indicating greater quantity and/or severity of inattention and hyperactivity symptoms.

## 2.4. Experimental paradigm

A visuospatial discrimination task, termed Vis-Attend, was used to engage the visuospatial processing circuitry (Fung et al., 2020, 2022; Killanin et al., 2020; Wiesman et al., 2017; Fig. 1). During this task, participants were told to fixate on a centrally presented crosshair. After a variable interstimulus interval (range: 1900–2100 ms), an  $8 \times 8$  grid was presented for 800 ms at one of four positions relative to the fixation: above and to the right, below right, above left, or below left. The left and right orientations were defined as a lateral offset of 75 % of the grid from the center of fixation. Participants were instructed to press a button with their right hand to indicate whether the grid was positioned to the left (index finger) or right (middle finger) of the fixation point upon presentation of the grid. Each participant performed 240 trials (60 of each possible target location) in a pseudo-randomized order concurrent with MEG recording. Responses with a reaction time 2.5 standard deviations above or below the participant's mean were excluded prior to averaging.

## 2.5. MEG data acquisition

Recordings were conducted in a two-layer magnetically shielded room. With an acquisition bandwidth of 0.1–330 Hz, neuromagnetic responses were sampled continuously at 1 kHz using a MEGIN Triux Neo MEG system with 306 magnetic sensors (Helsinki, Finland). MEG data from each participant were individually corrected for head motion and subjected to noise reduction using the signal space separation method with a temporal extension (Taulu et al., 2005; Taulu and Simola, 2006).

## 2.6. Structural MRI acquisition and coregistration with MEG data

Preceding MEG recording, five coils were attached to the participant's head and localized, together with the three fiducial points and scalp surface, with a 3D digitizer (Fastrak 3SF002; Polhemus Navigator Sciences, VT). Once the participant was positioned for MEG recording, an electric current with a unique frequency label (i.e., 322 Hz) was fed to each of the coils. This induced a measurable magnetic field and allowed each coil to be localized in reference to the sensors throughout the recording session. Since coil locations were also known in head coordinates, all MEG measurements could be transformed into a common coordinate system. With this coordinate system, each participant's MEG data were coregistered with their structural T1-weighted neuroanatomical data prior to source space analyses using BESA MRI (Version

3.0; BESA GmbH, Gräfelfing, Germany). Structural T1-weighted MR images were acquired using a Siemens Prisma 3 T MRI scanner with a 32-channel head coil and a MP-RAGE sequence with the following parameters: TR = 2400 ms; TE = 1.94 ms; flip angle =  $8^\circ$ ; FOV = 256 mm; slice thickness = 1 mm (no gap); voxel size =  $1 \times 1 \times 1$  mm. All structural MRI data were aligned parallel to the anterior and posterior commissures and transformed into standardized space, along with the functional images, after beamforming.

## 2.7. MEG time-frequency transformation and statistics

Cardiac and ocular artifacts (e.g., blinks, eye movement) were removed from the data using signal-space projection (SSP), which was accounted for during source reconstruction (Uusitalo and Ilmoniemi, 1997). MEG data were then analyzed with respect to stimulus onset to evaluate the oscillatory dynamics underlying visuospatial processing. To evaluate these dynamics, the continuous magnetic time series was divided into epochs of 2700 ms duration, with the baseline extending from  $-400$ – $0$  ms before stimulus onset (i.e., appearance of the checkerboard). Note that the baseline period was selected to prevent motor responses from the prior trial from “contaminating” the baseline. Epochs containing artifacts were rejected based on a fixed threshold method, supplemented with visual inspection. In brief, for each individual, the distribution of amplitude and gradient values was computed across all trials, and those trials containing the highest amplitude and/or gradient values relative to the full distribution were rejected by selecting a threshold that excluded extreme values. Importantly, these thresholds were set individually for each participant, as interindividual differences in variables such as head size and proximity to the sensors strongly affect MEG signal amplitude. On average,  $193.88 \pm 18.37$  trials per participant remained after artifact rejection. We determined whether the number of trials remaining in each condition varied as a function of any of our predictors of interest (i.e., age, radon exposure, and their interaction) using a multiple regression with mean centered variables. We did note a significant main effect of age ( $\beta = .57$ ,  $b = 4.58$ ,  $t = 2.27$ ,  $p = .025$ ), such that older children tended to have more trials than younger children. There were no other significant associations ( $p$ s = .61, .78). Because of this potential confounding effect of the number of trials on age-related effects of interest, we did covary the square root of the number of trials per person in all subsequent analyses of neural dynamics to adjust for differences in signal-to-noise ratio that may be present in the data (Gross et al., 2013; Junghöfer et al., 2000; Pulliam

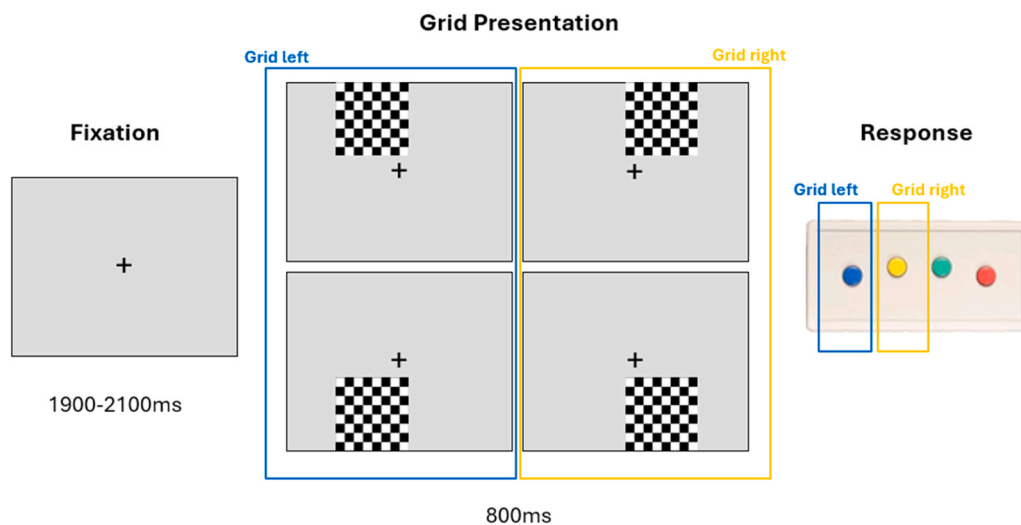


**Fig. 1.** Visuospatial task paradigm (Vis-Attend). Each trial consisted of a fixation lasting an average of 2000 ms (1900–2100 ms variable ISI), and an 800 ms stimulus-presentation period with the grid appearing in one of four locations. Participants indicated the location of the stimulus grid relative to the fixation with a button press (left or right).

et al., 2024; Vincent, 1992).

Artifact-free epochs were transformed into the time–frequency domain using complex demodulation with a resolution of 2 Hz and 25 ms, and the resulting spectral power estimations per sensor were averaged across all trials to generate time–frequency plots of mean spectral density. These sensor-level data were then normalized with respect to baseline power, which was calculated as the mean power between –400 and 0 ms prior to stimulus onset. Of note, this normalization was performed separately for each 2 Hz by 25 ms bin within each spectrogram using the corresponding baseline data.

The time–frequency windows used for imaging were determined by statistical analysis of the sensor-level spectrograms across all trials, gradiometers, and participants. Each data point (i.e., 2 Hz by 25 ms bin) in the spectrogram was initially evaluated using a mass univariate approach based on the general linear model. To reduce the risk of false positive results while maintaining reasonable sensitivity, a two-stage procedure was followed to control for Type 1 error. In the first stage, paired-sample *t*-tests against baseline were conducted on each data point and the output spectrogram of *t* values was thresholded at  $p < .05$  to define time–frequency bins containing potentially significant oscillatory deviations across all participants. In stage two, time–frequency bins that survived this threshold were clustered with temporally and/or spectrally neighboring bins that were also significant, and a cluster value was derived by summing all the *t* values of all data points in the cluster. Nonparametric permutation testing was then used to derive a distribution of cluster values and the significance level of the observed clusters (from stage one) were tested directly using this distribution (Ernst, 2004; Maris and Oostenveld, 2007). For each comparison, 1000 permutations were computed to build a distribution of cluster values. Based on these analyses, only the time–frequency windows that contained significant oscillatory events across all trials were subjected to the beamforming (i.e., imaging) analysis. Thus, a data-driven approach was utilized for selecting the time–frequency windows to be imaged.

## 2.8. MEG source imaging and statistics

Cortical dynamics were imaged through an extension of the linearly constrained minimum variance vector beamformer (Gross et al., 2001; Hillebrand et al., 2005; Van Veen et al., 1997), which applies spatial filters to time–frequency sensor data to calculate voxel-wise source power for the entire brain volume. Such images are typically referred to as pseudo-*t* maps, with units (pseudo-*t*) that reflect noise-normalized power differences (i.e., active vs. passive) per voxel. Following convention, the source power in these images was normalized per participant using a separately averaged pre-stimulus noise period (i.e., baseline) of equal duration and bandwidth (Hillebrand et al., 2005). MEG preprocessing and imaging used the Brain Electrical Source Analysis (version 7.1) software.

Normalized source power was computed for the selected time–frequency bands over the entire brain volume per participant at  $4.0 \times 4.0 \times 4.0$  mm resolution. Each participant’s functional images were transformed into standardized space using the transform that was previously applied to the structural images and then spatially resampled. The resulting 3D maps of brain activity were examined for potential outliers, identified as maps containing clusters with pseudo-*t* values exceeding  $\pm 3.0$  standard deviations about mean. Such outliers are often the result of artifacts that could not be removed in our rigorous preprocessing scheme and interfere with accurate source reconstruction during beamforming. The remaining maps after outlier exclusions were grand averaged across participants to assess the anatomical basis of the significant oscillatory responses identified through the sensor-level analysis.

To assess associations between chronic everyday home radon exposure, age, and neural oscillatory dynamics, we computed whole-brain linear regressions (one for each of the oscillatory bands of interest) with the radon exposure index, age, and their interaction as predictors of

interest, and the map of brain activity for each oscillatory band as the dependent measure of interest. We mean-centered our predictors to account for potential multicollinearity considering the interaction term. Signal-to-noise ratio (SNR), computed as the square-root of the total number of trials per person, was included as a covariate of no interest to adjust for potential differences in the number of trials across individuals. To account for multiple comparisons, a significance threshold of at least  $p < 0.001$  was used for the identification of significant clusters in all whole-brain statistical maps, accompanied with a stringent cluster (*k*) threshold of more than 5 contiguous voxels of  $4.0 \times 4.0 \times 4.0$  mm (i.e., at least 320 mm<sup>3</sup>). These analyses, performed in SPM 12, yielded *F* maps showing significant clusters with main effects of age, radon exposure, and their interaction. We report the standardized beta coefficients for significant associations identified in the *F* maps for interpretability of the effects. Pseudo-*t* values were extracted from the peak voxels of each significant cluster per participant to further probe effects of interest. In particular, we used the Interactions (Long, 2019) and JTools (Long, 2022) packages in R (version 4.3.3) to probe age-by-radon interactions using simple slopes analysis. Of note, because the current investigation is focused on the effects of radon exposure, only the main effects of radon and the radon-by-age interaction are reported here. Effects of age have been reported previously (Killanin et al., 2020).

Finally, we performed mediation analyses to test the degree to which radon-related aberrations in the neural oscillatory dynamics serving visuospatial processing were functionally relevant. We specifically explored whether clusters showing radon-related aberrations subsequently predicted either task performance (i.e., reaction time and accuracy) or attentional symptoms (i.e., raw Inattention/Hyperactivity scores from the BASC-3). Because traditional tests of indirect effects (e.g., the Sobel test) often violate the assumption of normality, we utilized asymmetrical confidence intervals which best represent the true distribution of the indirect effect (i.e., the product of coefficients from the “a” and “b” paths). Thus, we examined the 95 % confidence intervals of bias-corrected bootstrapped confidence intervals based on 1000 bootstrapped samples to more rigorously detect any potential relationships between brain activity and behavior (Austin and Tu, 2004; Efron and Tibshirani, 1986; Fritz and MacKinnon, 2007), which provide a robust estimate of mediation effects and are asymmetrical (Fritz and MacKinnon, 2007). Mediation analyses were conducted in JASP version 18.3.

## 3. Results

### 3.1. Behavioral analysis

Of the 118 youths who consented to the study, five did not complete the MEG scan, three had incomplete or unreturned radon test results, two did not complete the home radon questionnaire, and three were excluded due to technical errors during MEG recording. Of the remaining 105 participants, two were excluded from further analyses due to low accuracy (less than 60 % correct) on the VisAttend task. Thus, the final sample consisted of 103 children and adolescents ( $M = 12.22 \pm 2.27$  years, 51 males). Participants performed well on the visuospatial processing task. The average accuracy was  $90.37\% \pm 7.33\%$  and the average reaction time was  $611.55 \pm 138.87$  ms. Using two separate multiple regression analyses, we determined whether there were any associations between the measures of interest (i.e., age, radon exposure, and their interaction) and either accuracy or reaction time on the task. As expected, there was a main effect of age on accuracy ( $\beta = .53$ ,  $b = 1.73$ ,  $t = 2.16$ ,  $p = .033$ ) with older children generally having higher task accuracy relative to their younger peers. We did not find any other statistically significant associations.

### 3.2. Home radon exposure

Home radon concentrations ranged from 0.2 to 12.2 pCi/L with an average of 3.79 pCi/L ( $SD = 2.86$ ). Every family also reported how long

the children had lived in their current home. Participants were exposed to the recorded radon level for an average of 6.95 years (SD = 3.81, range = 0.08–15 years). As stated in the Methods, we computed a radon exposure index for each participant by combining the recorded home radon concentration and the duration of time that the child had lived in their home. The resultant radon exposure index had an average of 2.87 (SD = 1.09), ranging from 0.11 to 4.98.

### 3.3. Sensor-level analysis

Statistical analysis of the stimulus-locked time-frequency spectrograms revealed five significant clusters of oscillatory activity (Fig. 2, all  $p$ s < .001 after cluster-based permutation testing), representing the neural oscillatory responses to the task. Significant synchronizations, or increases in power relative to baseline, were observed in the theta band (4–8 Hz) from 50 to 300 ms, and in the gamma range during an early (100–175 ms, 70–88 Hz) and later (325–575 ms, 66–82 Hz) window in posterior sensors. A significant decrease in power, or event-related desynchronization (ERD), was observed in the alpha band (8–14 Hz) from 375 to 625 ms, and in the beta band (18–24 Hz) from 350 to 550 ms in posterior sensors.

### 3.4. Beamformer analysis

To identify the brain regions generating significant sensor-level oscillations, these time frequency windows were imaged using a beamformer. These source level images were then examined for outliers, with significant artifactual or excessively noisy data excluded. This left 88 participants with evaluable data in the theta band, 97 in alpha, 94 in beta, 94 in early gamma, and 98 in late gamma. The resulting maps were grand averaged across participants, and these responses are shown in Fig. 2. Strong oscillatory responses were observed across all bands in bilateral visual cortices, as expected for the visual processing task.

### 3.5. Radon-by-age interaction

For each oscillatory response, individual beamformer maps were submitted to whole-brain multiple linear regression analyses to explore the effects of age, radon, and the age-by-radon interaction on neural

dynamics, controlling for SNR. Although we did not detect any main effects of radon, we did find significant age-by-radon interactions.

In the beta band, our whole-brain linear regression revealed significant age-by-radon interactions in the left inferior frontal gyrus (IFG;  $F = 13.87$ ,  $p < .001$ ,  $\eta_p^2 = 0.14$ ) and left superior temporal gyrus (STG;  $F = 15.06$ ,  $p < .001$ ,  $\eta_p^2 = 0.15$ ). In both regions, youths with the lowest radon exposure (i.e.,  $-1$  SD REI) exhibited a beta ERD at age 8 that generally weakened with age, whereas those with the greatest radon exposure (i.e.,  $+1$  SD REI) showed limited beta ERD at age 8, though the response strengthened with age. Individuals with only moderate levels of radon exposure showed little to no change in beta ERD across development (Fig. 3).

### 3.6. Relationships to task behavior

We tested a moderated mediation model to determine whether radon exposure modulated the indirect effect of age on task behavior (i.e., reaction time and accuracy) via visuospatial beta dynamics in the left IFG and STG. Although we found no links to task accuracy, we did find significant moderated indirect effects on reaction times via both the left IFG ( $\beta = -.042$ , 95 % CI [-.099, -.010]; Fig. 4) and the left STG ( $\beta = -.041$ , 95 % CI [.010, .112]; Fig. 5).

In the left IFG, children with relatively high levels of radon exposure (i.e.,  $+1$  SD REI) showed little-to-no recruitment of the left IFG at younger ages, but progressively showed stronger beta ERD with increasing age ( $b = -7.27$ , 95 % CI [-16.77, -1.15]; Fig. 4B). Among these youth, stronger beta ERDs were predictive of slower reaction times during the task (Fig. 4C). Conversely, those with relatively low radon exposure (i.e.,  $-1$  SD REI) showed strong beta ERD in the left IFG at a younger age, which weakened across development. Stronger beta ERDs were linked with slightly faster reaction times among these youth, though the effect was relatively weak ( $b = 1.12$ , 95 % CI [0.062, 15.43]; Fig. 4C).

In the left STG, the conditional effect of radon was specific to cases of higher exposure (i.e.,  $+1$  SD REI;  $b = 1.12$ , 95 % CI [0.87, 19.61]). We saw that youth with the greatest degree of radon exposure had little-to-no beta ERD in the left STG at younger ages, but there was a progressively stronger ERD as a function of increasing age. Among these youth, stronger beta ERD in the STG was predictive of slower reaction times on

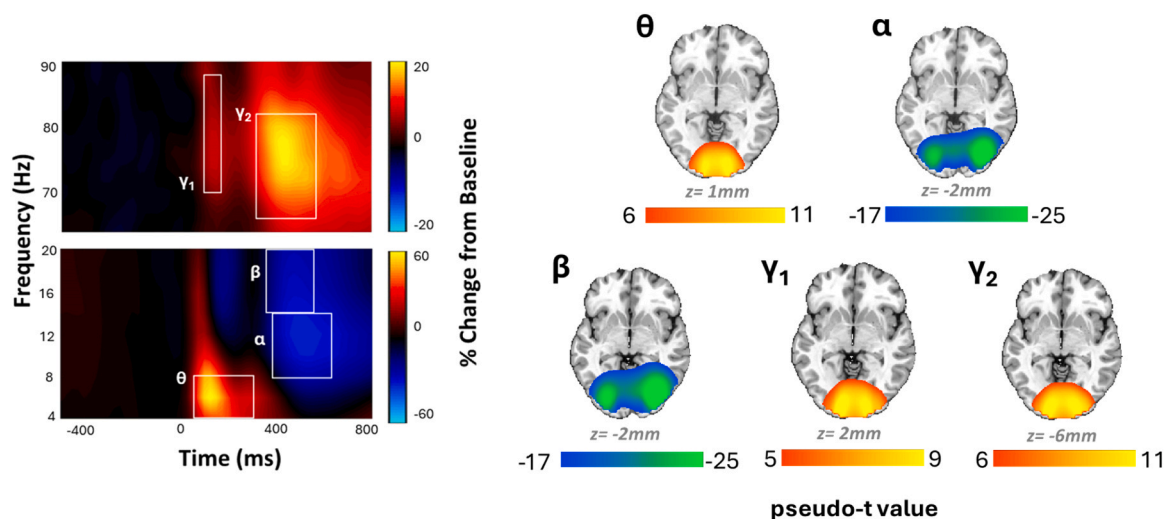


**Fig. 2.** Spectrograms of significant oscillatory responses during the task and source reconstructions. Left panel: Time-frequency decomposition and permutation-corrected statistical analyses indicated five time-frequency bins with significant responses relative to baseline (marked by white boxes). These included theta, alpha, beta, and early and late gamma activity. While statistical analyses included all gradiometers, the occipital sensor that most clearly showed the responses is shown above (i.e., MEG 2342). Warm colors reflect power increases relative to the baseline, and cool colors represent decreases relative to baseline. Right panel: Whole brain visualizations of the origin of oscillatory responses within each frequency band. Each map is a grand average across all participants. Across all bands, oscillatory responses were strongest in bilateral visual cortices. Color scale bars indicate the strength of responses (pseudo-t). Warm colors indicate synchronizations; cool colors indicate desynchronizations.

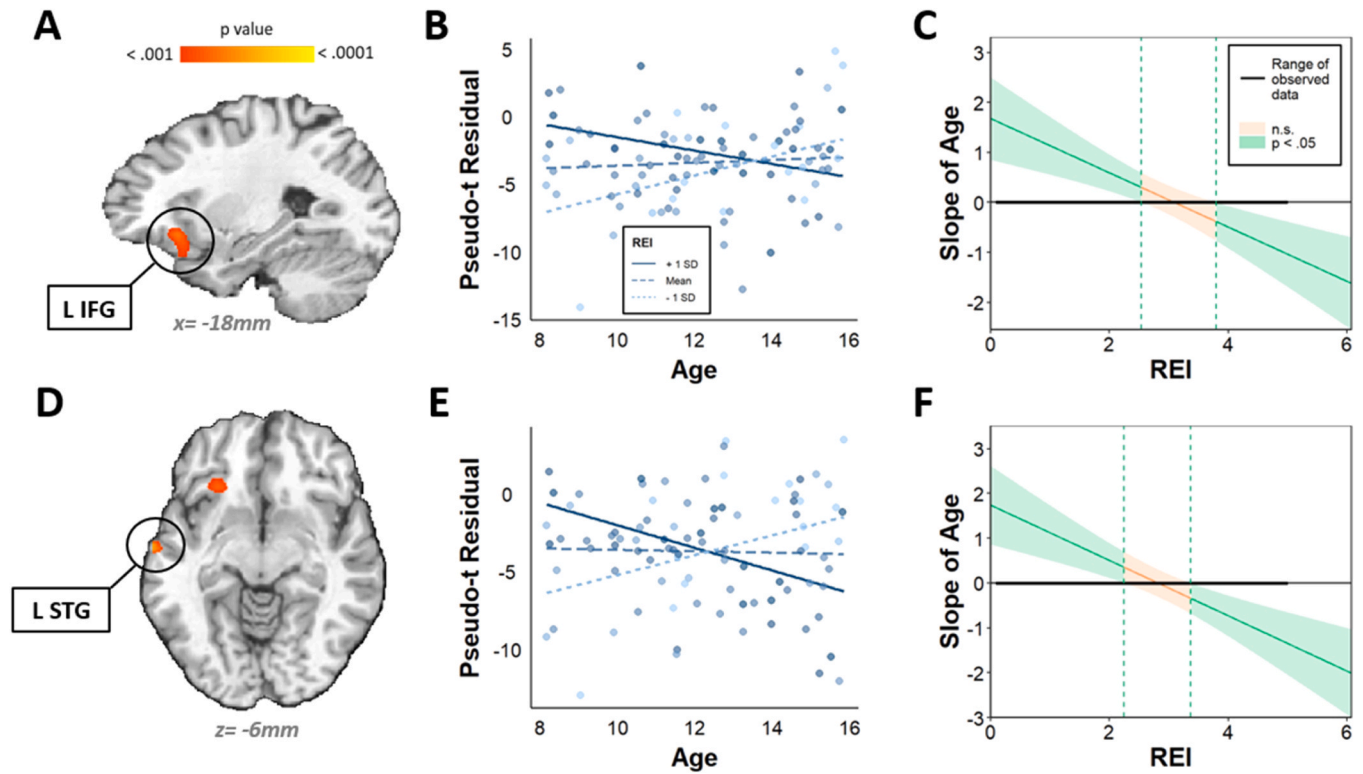


**Fig. 3.** Age-by-radon interactions on visuospatial oscillatory dynamics within the beta band. A, D: Statistical F maps showing clusters for which there was a statistically significant age-by-radon exposure interaction. B, E: Scatterplots showing the differential association between age and the beta response for the mean  $\pm$  1 SD radon exposure index, with  $-1$  SD being relatively low radon exposure, the mean being moderate radon exposure, and  $+1$  SD being relatively high radon exposure. The pseudo-t values are residuals after accounting for SNR. C, F: Johnson-Neyman plots showing the levels of radon exposure index for which there is a significant interaction effect. Notes: “L” = left; “IFG” = inferior frontal gyrus; “REI” = radon exposure index; “STG” = superior temporal gyrus.

the visuospatial task.

### 3.7. Relationships to attentional symptoms

In a second analysis, we investigated whether radon exposure modulated the indirect effect of age on attentional symptoms via beta dynamics in the left IFG and STG. Self-reported raw Inattention/Hyperactivity scores from the BASC-3 in our sample ranged from 0 to 23, with the average being  $8.04 \pm 4.72$ .

We found that radon exposure modulated the indirect effect of age on inattention/hyperactivity symptoms via beta dynamics in the left IFG (Fig. 6,  $\beta = -.050$ , 95 % CI  $[-.114, -.012]$ ), and this conditional effect was specific to youths with higher levels of radon exposure (i.e.,  $+1$  SD REI;  $b = -.021$ , 95 % CI  $[-0.49, -0.024]$ ). Children with relatively high levels of radon exposure showed little-to-no recruitment of the left IFG at younger ages, but progressively showed stronger beta ERD with increasing age. Among these youth, stronger beta ERDs were predictive of less self-reported difficulties with inattention and hyperactivity (i.e., lesser ADHD symptomatology).

## 4. Discussion

The goal of the present study was to elucidate the impact of chronic home radon exposure on the developmental trajectory of neural oscillatory dynamics serving visuospatial attention, and to understand whether these radon-related alterations to dynamics were behaviorally relevant. In support of our hypothesis, we found that radon exposure significantly modulated the maturation of oscillatory dynamics within two neural substrates that play a critical role in visuospatial attention: the left STG and IFG. Crucially, we found that these radon-related alterations to expected developmental trajectories were functionally

relevant. In both areas, youths with the highest radon exposure exhibited stronger beta responses as a function of age, and these stronger beta responses predicted slower visuospatial task reaction times. Strikingly, in the left IFG we found that age-related increases in beta responses among youths exposed to the highest levels of radon were correlated with lesser ADHD symptomatology. Each of these novel findings and their implications are discussed below.

Within both the left IFG and left STG, youths with the highest radon exposure (i.e.,  $+1$  SD REI) exhibited significantly stronger beta ERDs as a function of increasing age, which predicted *slower* reaction times on the visuospatial task. Those with the lowest levels of exposure (i.e.,  $-1$  SD REI) exhibited the opposite pattern, with beta ERDs weakening as youths matured. According to the Neural Efficiency Hypothesis, greater cognitive ability is associated with more efficient brain activation, whereby less neural activity is needed to complete a task (Neubauer and Fink, 2009). From this perspective, age-related weakening of beta ERD in the lowest exposure group may reflect healthy development, indicating greater efficiency as networks mature and fewer resources are required for task completion. A similar pattern has been observed in the typical developmental course of visuospatial theta oscillatory dynamics, whereby decreasing activation with age is associated with greater network maturity (Fung et al., 2022). In contrast, the age-related strengthening of beta responses in youths with high radon exposure may reflect reduced neural efficiency, potentially signaling underlying neurocognitive deficits that result in an alternate cognitive strategy. This interpretation is in line with other studies that have found overly strong oscillatory responses associated with environmental exposures to reflect more effortful processing to sustain performance relative to lesser-exposed peers (D. Guo et al., 2022; Pulliam et al., 2024).

In youths exposed to high levels of radon, stronger beta ERDs in the left IFG were associated with slower reaction times and *lesser* inattention

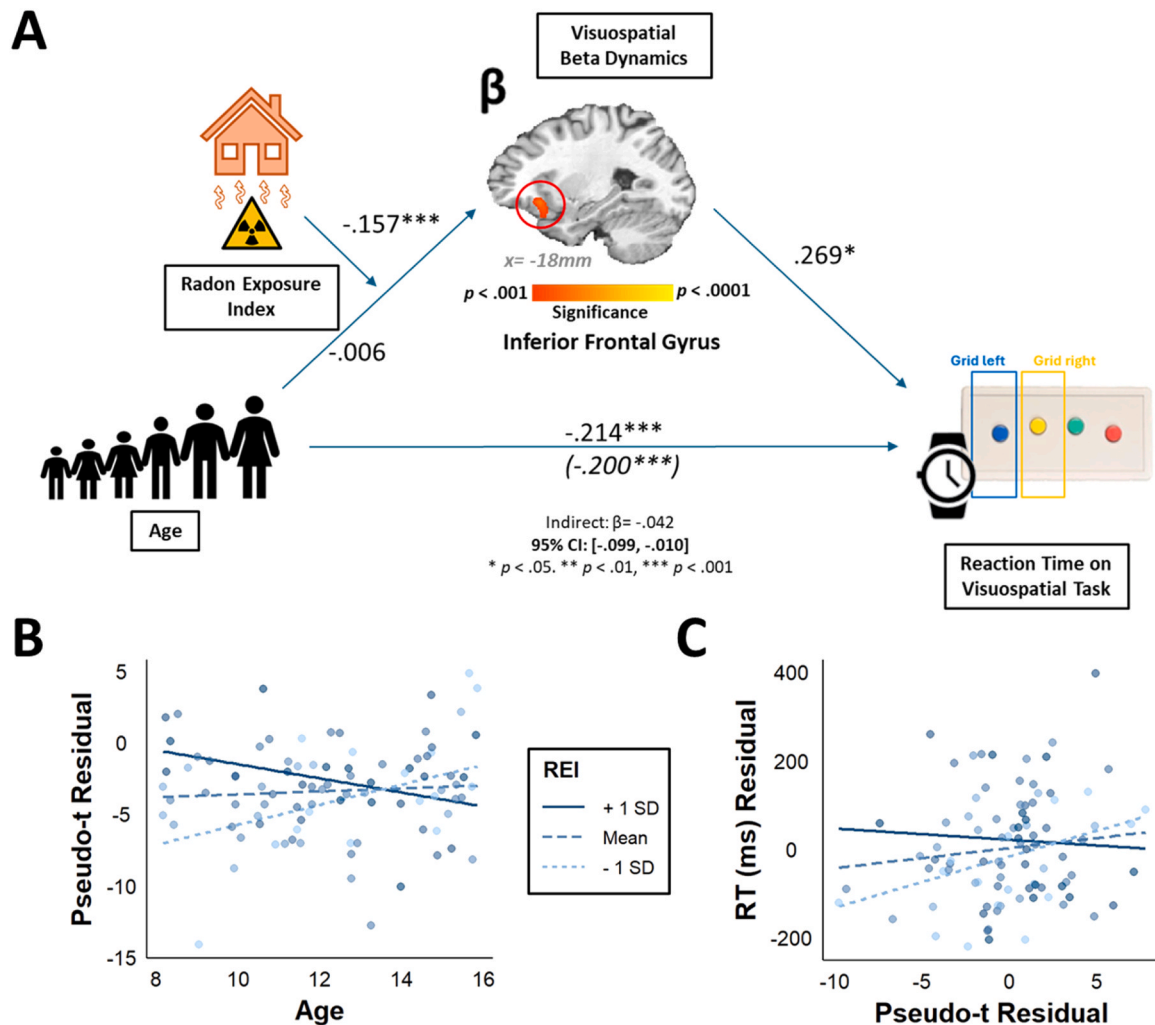


**Fig. 4.** A: Moderated mediation model wherein radon exposure is a modulator of the indirect effect of age on reaction time via aberrant beta dynamics in the left IFG. B: Scatterplot showing the differential association between age and the beta response for the mean  $\pm$  1 SD radon exposure index. Pseudo-t values are residuals after accounting for the effect of SNR and age; reaction times are residuals accounting for the effect of age. Children with high radon exposure show stronger beta responses with age (B); those stronger beta responses predicted slower reaction times on the task (C). Those with low radon exposure show weaker beta responses with age (B); stronger beta responses in these youth are weakly linked with faster reaction times (C).

and hyperactivity symptoms. The left IFG has roles in focusing spatial attention, inhibitory control, and filtering out task-irrelevant information (Chong et al., 2008; Corbetta and Shulman, 2002; Swick et al., 2008; Vossel et al., 2014). The importance of this region in attention functioning is underscored by a large body of clinical work that ties left IFG dysfunction to ADHD (Chen et al., 2025; Chevrier and Schachar, 2020; Cortese et al., 2016; Li et al., 2023; Nickel et al., 2018; Samea et al., 2019; Van Ewijk et al., 2015; Wang et al., 2013). Thus, our findings are well-aligned with a growing body of work linking environmental exposures to ADHD, both with respect to clinically diagnosed disorders (Aghaei et al., 2019; Bernardina Dalla et al., 2022; Min and Min, 2017; Myhre et al., 2018; Newman et al., 2013; Peterson et al., 2015; Thapar et al., 2013; Thygesen et al., 2020), and subclinical symptomologies (T. Guo et al., 2025; Herting et al., 2024; Rauh and Margolis, 2016; Wylie and Short, 2023). Indeed, toxic exposures have been linked to subclinical attention symptoms and dysfunction even in typically-developing populations (Castagna et al., 2022; Compa et al., 2023; D. Guo et al., 2022), and evidence associating environmental toxicants with subclinical effects and symptomology, such as those seen in our sample of typically-developing youths, is vitally important in characterizing the impact of these exposures (Rauh and Margolis, 2016).

In addition to the left IFG, we observed radon-related aberrations in beta oscillatory dynamics of the left STG, which has been implicated in attentional functions such as contextual updating (Geng and Vossel, 2013). The left IFG and left STG overlap with the ventral frontal cortex (VFC) and temporoparietal junction (TPJ), respectively, which are key nodes of the VAN that are functionally connected and frequently coactivated (Corbetta and Shulman, 2002; Farrant and Uddin, 2015). Interestingly, the VAN is typically understood to be primarily right-lateralized. It is possible that the observed aberrations in our sample represent compensatory recruitment of left hemisphere attentional regions to maintain cognitive performance despite chronic environmental insult. Furthermore, exposures to inhaled environmental toxicants have been found to alter connectivity between and within networks serving higher-order cognitive functions (Cotter et al., 2023; Kusters et al., 2025). This is important when considering that efficient visuospatial attentional allocation is dependent on a dynamic balance of VAN/DAN interactions (Vossel et al., 2014). The IFG and STG have been implicated in governing this interplay (Solís-Vivanco et al., 2021; Vossel et al., 2014), and beta oscillations have been suggested to play a role in modulating these interactions (Solís-Vivanco et al., 2021). Increased beta recruitment of left-lateralized regions in youths with high radon

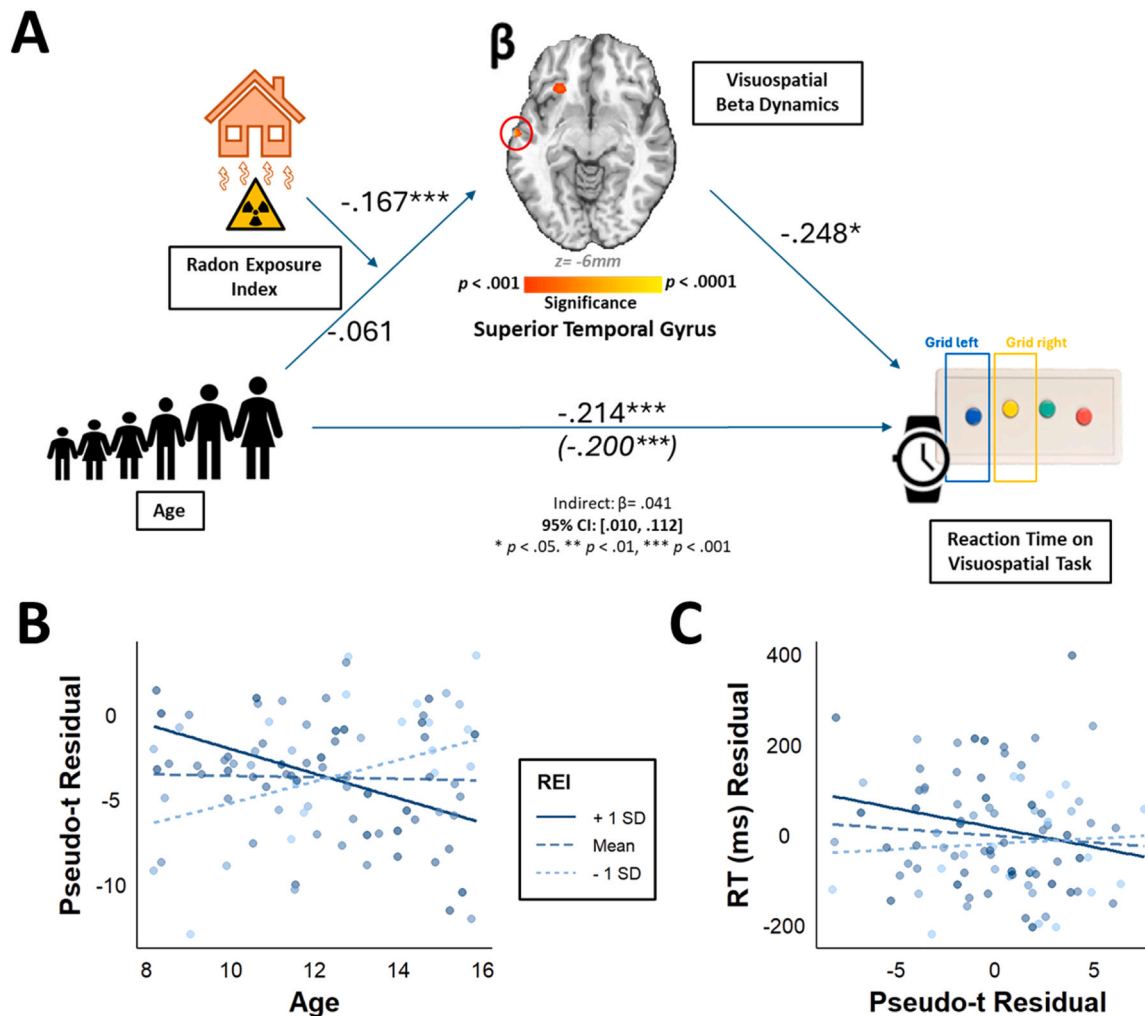


**Fig. 5.** **A:** Moderated mediation model wherein radon exposure is a modulator of the indirect effect of age on reaction time via aberrant beta dynamics in the left STG. **B:** Scatterplot showing the differential association between age and the beta response for the mean  $\pm 1$  SD radon exposure index. Pseudo-t values are residuals after accounting for the effect of SNR. **C:** Scatterplot showing the relationship between the STG beta response and reaction time. Pseudo-t values are residuals after accounting for the effect of SNR and age; reaction times are residuals accounting for the effect of age. Children with high radon exposure show stronger beta responses with age (B); these stronger beta responses in the left STG predicted slower reaction times on the visuospatial task (C).

exposure may disrupt typical VAN/DAN interactions, leading to dysregulated engagement of attentional systems. Future works could consider exploring connectivity approaches to further probe this potential explanation.

Interestingly, our radon-related findings were confined to effects in the beta band. In the context of attention functioning, beta activity has been associated with top-down control, activation of attentional systems, and maintenance of sustained attention (Benchenane et al., 2011; Di Dona and Ronconi, 2023; Gola et al., 2013; Güntekin et al., 2013; Taylor et al., 2025; Wróbel, 2000). In clinical contexts such as Parkinsonism, excessive beta activity is associated with impaired movement (Brown, 2007). Dopaminergic medications that suppress beta synchrony improve motor flexibility and also exert effects on top-down attention processes (Jiang et al., 2024), suggesting a role for beta activity in the maintenance of cognitive and motor sets. Indeed, increases in beta power are associated with top-down inhibition that maintains a stable set, whereas decreases in beta activity are thought to reflect the disruption of that set to adapt to novel or unexpected stimuli (Engel and Fries, 2010). Building from this idea, stronger beta ERD in the left IFG may reflect increased top-down control and a tendency to hold onto current representations, which may slow the ability to flexibly shift attention and respond quickly to new stimuli during the task. It makes sense that this greater top-down control would help reduce ADHD

symptomology by improving attentional stability; though it appears to come at the cost of decreased flexibility and less efficient processing, as evidenced by longer reaction times and greater neural effort compared to lesser-exposed peers. Thus, these age-related increases in beta ERD may indicate compensatory activity that sacrifices some efficiency of processing for better behavioral outcomes (i.e., lesser inattention and hyperactivity symptoms). This interpretation is in line with another prior study positing that, rather than solely being devoted to task performance, altered activity in the left IFG may reflect the allocation of neural resources to actively manage symptomatic behavior (Chevrier and Schachar, 2020). It is further supported by another study in which greater beta activity was negatively correlated with symptoms of inattention and hyperactivity in typically-developing children (Bocharov et al., 2021).

The oscillatory dynamics underlying attention-related networks, including the DAN and VAN, undergo significant developmental changes throughout childhood and adolescence (Fung et al., 2020, 2022; Killanin et al., 2020; Picci et al., 2023; Taylor et al., 2021). This period of heightened plasticity is critical for the maturation of stable and efficient attentional systems (Abundis-Gutiérrez et al., 2014; Dong et al., 2024; Farrant and Uddin, 2015; Konrad et al., 2005; Schul et al., 2003), but also represents a window of vulnerability during which the brain is particularly susceptible to harmful environmental exposures (Bearer,

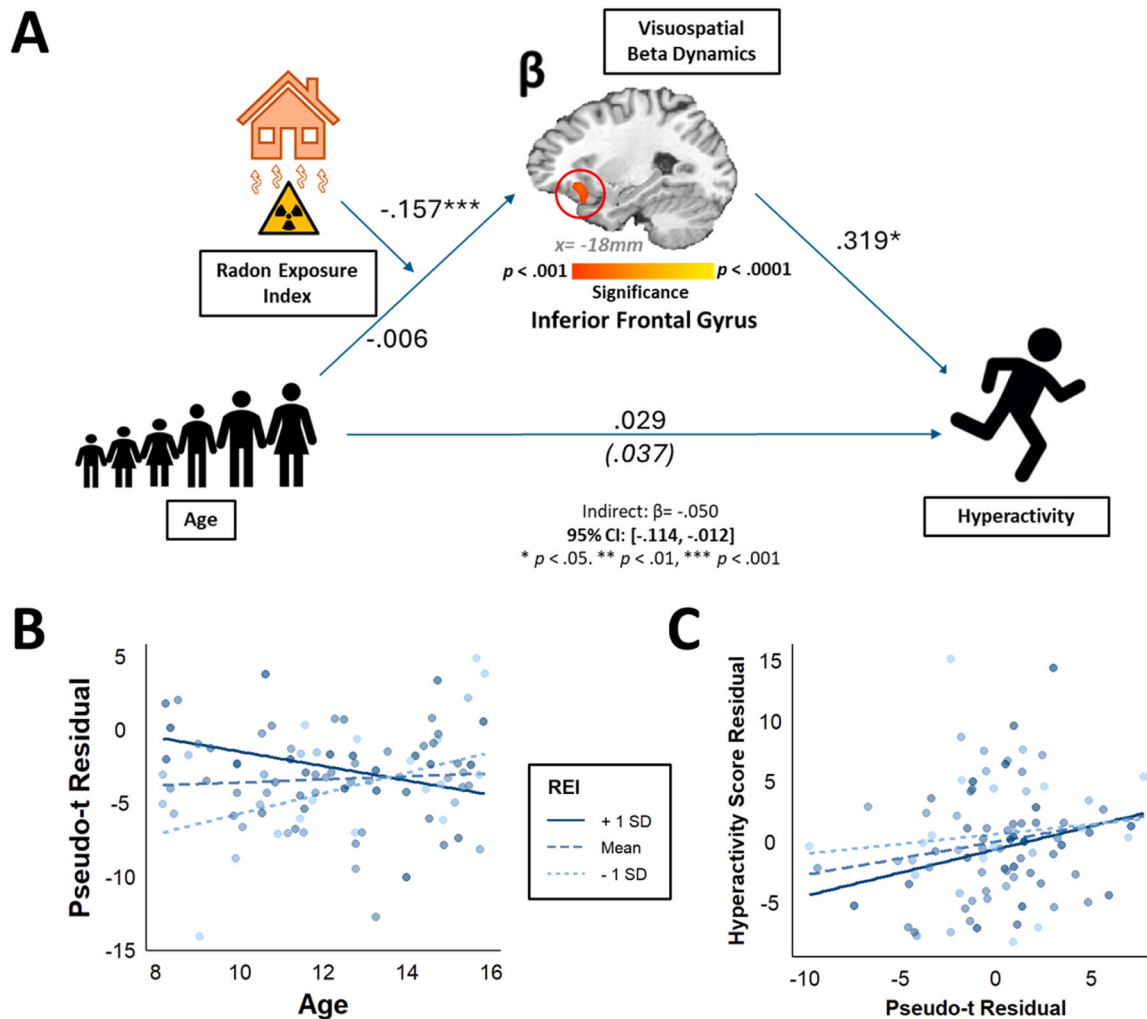


**Fig. 6.** A: Moderated mediation model wherein radon exposure is a modulator of the indirect effect of age on hyperactivity scores via aberrant beta dynamics in the left IFG. B: Scatterplot showing the differential association between age and the beta response for the mean  $\pm$  1 SD radon exposure index. Pseudo-t values are residuals after accounting for the effect of SNR. C: Scatterplot showing the impact of the left IFG beta response on hyperactivity scores. Pseudo-t values are residuals after accounting for the effect of SNR and age; hyperactivity score values are residuals accounting for the effect of age.

1995; Goldman, 1995; Perera et al., 2006). Radon exposure among youths has been previously linked to alterations in oscillatory dynamics underlying attentional reorienting (Pulliam et al., 2024), suggesting that radon may contribute to attention dysfunction by altering developmental trajectories of cortical oscillatory patterning. By uncovering radon-related alterations in the neurodevelopmental trajectories of visuospatial attention networks and establishing a link between these alterations and attention symptomology in youth, we extend this important work and complement other evidence characterizing radon’s toxic neurodevelopmental effects (Smith et al., 2024; Taylor et al., 2024, 2022).

Before closing, we must acknowledge several limitations of the current study. First, the observational, cross-sectional design of our study prevents conclusions about temporal relationships and causality. Future longitudinal research is needed to clarify how radon exposure may influence the developmental trajectory of visuospatial oscillatory dynamics and their relationship to ADHD symptoms over time. Second, we relied on self-reported inattention and hyperactivity scores from the BASC-3, which may yield different results than teacher- or parent-reported measures (Du Rietz et al., 2016; Slobodin and Davidovitch, 2022). Future studies should incorporate multiple informants and standardized clinical tools (e.g., DSM-5 criteria, Conners Rating Scale, CPT, or ADHD Rating Scale) to more accurately assess ADHD

symptomology. Third, we did not consider multiple exposures, and it is possible that radon has interactive effects with other toxins and toxicants. It would be beneficial to consider the potential combined or synergistic effects of radon with other common toxicants like particulate matter. Fourth, home radon testing was conducted over a period of 30 days in the current study, which is generally considered more acute. Longer testing periods (e.g., 90days or greater) may provide more stable measurements of long-term home radon levels. It would be beneficial to explore longer term testing in future studies to ensure the most robust measurements possible. Finally, although our use of long-term home radon kits provided reliable exposure data, we did not account for radon exposure in other environments, such as schools, which may contribute to overall exposure. Acquiring additional measurements from other frequently-attended locations, as well as historical data (e.g., former residences) would enrich the analysis of cumulative lifetime radon exposure.

4.1. Conclusion

To conclude, the findings of this study contribute to a broader body of work showing that environmental radon exposure is capable of impacting brain development in cognitively, behaviorally, and clinically relevant ways. In a large sample of typically-developing youth, we found

radon-related aberrations to developmental trajectories of neural beta oscillations serving visuospatial attentional abilities in the left IFG and STG. In youths with high radon exposure, alterations to these trajectories were predictive of slower task reaction time, and, in the left IFG, they were additionally associated with lesser self-reported inattention and hyperactivity symptoms. Our results implicate radon as a potential neurotoxin linked with critical alterations to oscillatory dynamics within brain networks paramount to high-order cognition. These altered developmental trajectories may represent patterns of compensatory neural activity to sustain performance and promote better behavioral outcomes despite chronic environmental insult.

## Funding

This work was supported by the National Institutes of Health (P20-GM144641 and R21-ES035146 to BKT). The funders had no part in the study design, analysis, interpretation, or writing of this report.

## CRedit authorship contribution statement

**OgheneTejiri V. Smith:** Writing – review & editing, Investigation, Data curation. **Haley R. Pulliam:** Writing – review & editing, Investigation, Data curation. **Brittany K. Taylor:** Writing – review & editing, Supervision, Project administration, Methodology, Funding acquisition, Conceptualization. **Danielle Thompson:** Writing – review & editing, Visualization, Formal analysis. **Monica N. Clarke-Smith:** Writing – review & editing, Investigation, Data curation. **Saige C. Rasmussen:** Writing – review & editing, Investigation, Data curation. **Grace E. Parolek:** Writing – review & editing, Investigation, Data curation. **Sarah L. Greenwood:** Writing – review & editing, Visualization, Investigation, Formal analysis, Data curation. **Rachel A. Bonney:** Writing – review & editing, Writing – original draft, Visualization, Formal analysis.

## Declaration of Competing Interest

The authors declare that they have no known competing financial interests or personal relationships that could have appeared to influence the work reported in this paper.

## Acknowledgements

The authors would like to thank the families who participated in this study.

## Data availability

Data will be made available on request.

## References

Abundis-Gutiérrez, A., Checa, P., Castellanos, C., Rosario Rueda, M., 2014. Electrophysiological correlates of attention networks in childhood and early adulthood. *Neuropsychologia* 57, 78–92. <https://doi.org/10.1016/j.neuropsychologia.2014.02.013>.

Aghaei, M., Janjani, H., Yousefian, F., Jamal, A., Yunesian, M., 2019. Association between ambient gaseous and particulate air pollutants and attention deficit hyperactivity disorder (ADHD) in children; a systematic review. *Environ. Res.* 173, 135–156. <https://doi.org/10.1016/j.envres.2019.03.030>.

Austin, P.C., Tu, J.V., 2004. Bootstrap methods for developing predictive models. *Am. Stat.* 58 (2), 131–137. <https://doi.org/10.1198/0003130043277>.

Bearer, C.F., 1995. Environmental health hazards: how children are different from adults. *Future Child.* 5 (2), 11–26. <https://doi.org/10.2307/1602354>.

Beckwith, T., Cecil, K., Altaye, M., Severs, R., Wolfe, C., Percy, Z., Maloney, T., Yoltan, K., LeMasters, G., Brunst, K., Ryan, P., 2020. Reduced gray matter volume and cortical thickness associated with traffic-related air pollution in a longitudinally studied pediatric cohort. *PLoS ONE* 15 (1), e0228092. <https://doi.org/10.1371/journal.pone.0228092>.

Benchenane, K., Tiesinga, P.H., Battaglia, F.P., 2011. Oscillations in the prefrontal cortex: a gateway to memory and attention. *Curr. Opin. Neurobiol.* 21 (3), 475–485. <https://doi.org/10.1016/j.conb.2011.01.004>.

Bernardina Dalla, M.D., Ayala, C.O., Cristina de Abreu Quintela Castro, F., Neto, F.K., Zanirati, G., Cañon-Montañez, W., Mattiello, R., 2022. Environmental pollution and attention deficit hyperactivity disorder: a meta-analysis of cohort studies. *Environ. Pollut. (Barking Essex 1987)* 315, 120351. <https://doi.org/10.1016/j.envpol.2022.120351>.

Bisley, J.W., 2011. The neural basis of visual attention. *J. Physiol.* 589 (Pt 1), 49–57. <https://doi.org/10.1113/jphysiol.2010.192666>.

Bocharov, A.V., Savostyanov, A.N., Slobodskaya, H.R., Tamozhnikov, S.S., Levin, E.A., Saprygin, A.E., Proshina, E.A., Astakhova, T.N., Merkulova, E.A., Knyazev, G.G., 2021. Associations of hyperactivity and inattention scores with theta and beta oscillatory dynamics of EEG in stop-signal task in healthy children 7–10 years old. *Article 10. Biology* 10 (10). <https://doi.org/10.3390/biology10100946>.

Brown, P., 2007. Abnormal oscillatory synchronisation in the motor system leads to impaired movement. *Curr. Opin. Neurobiol.* 17 (6), 656–664. <https://doi.org/10.1016/j.conb.2007.12.001>.

Cardillo, R., Vio, C., Mammarella, I.C., 2020. A comparison of local-global visuospatial processing in autism spectrum disorder, nonverbal learning disability, ADHD and typical development. *Res. Dev. Disabil.* 103, 103682. <https://doi.org/10.1016/j.ridd.2020.103682>.

Castagna, A., Mascheroni, E., Fustinoni, S., Montiroso, R., 2022. Air pollution and neurodevelopmental skills in preschool- and school-aged children: a systematic review. *Neurosci. Biobehav. Rev.* 136, 104623. <https://doi.org/10.1016/j.neubiorev.2022.104623>.

Chen, C., Sun, S., Chen, R., Guo, Z., Tang, X., Chen, G., Chen, P., Tang, G., Huang, L., Wang, Y., 2025. A multimodal neuroimaging meta-analysis of functional and structural brain abnormalities in attention-deficit/hyperactivity disorder. *Prog. NeuroPsychopharmacol. Biol. Psychiatry* 136, 111199. <https://doi.org/10.1016/j.pnpbp.2024.111199>.

Chevrier, A., Schachar, R.J., 2020. BOLD differences normally attributed to inhibitory control predict symptoms, not task-directed inhibitory control in ADHD. *Article 1. J. Neurodev. Disord.* 12 (1). <https://doi.org/10.1186/s11689-020-09311-8>.

Chong, T.T.-J., Williams, M.A., Cunnington, R., Mattingley, J.B., 2008. Selective attention modulates inferior frontal gyrus activity during action observation. *NeuroImage* 40 (1), 298–307. <https://doi.org/10.1016/j.neuroimage.2007.11.030>.

Clement, C.H., Tirmarche, M., Harrison, J.D., Laurier, D., Paquet, F., Blanchardon, E., Marsh, J.W., 2010. Lung cancer risk from radon and progeny and statement on radon. *Ann. ICRP* 40 (1), 1–64. <https://doi.org/10.1016/j.icrp.2011.08.011>.

Compa, M., Baumbach, C., Kaczmarek-Majer, K., Buczyłowska, D., Gradyś, G.O., Skotak, K., Degórska, A., Bratkowski, J., Wierzbła-Lukaszyk, M., Mysak, Y., Sitnik-Warchulska, K., Lipowska, M., Izydorczyk, B., Grellier, J., Asanowicz, D., Markevych, I., Szwed, M., 2023. Air pollution and attention in Polish schoolchildren with and without ADHD. *Sci. Total Environ.* 892, 164759. <https://doi.org/10.1016/j.scitotenv.2023.164759>.

Corbetta, M., Shulman, G.L., 2002. Control of goal-directed and stimulus-driven attention in the brain. *Nat. Rev. Neurosci.* 3 (3), 201–215. <https://doi.org/10.1038/nrn755>.

Cortese, S., Castellanos, F.X., Eickhoff, C.R., D'Acunzio, G., Masi, G., Fox, P.T., Laird, A.R., Eickhoff, S.B., 2016. Functional decoding and meta-analytic connectivity modeling in adult attention-deficit/hyperactivity disorder. *Biol. Psychiatry* 80 (12), 896–904. <https://doi.org/10.1016/j.biopsych.2016.06.014>.

Cotter, D.L., Campbell, C.E., Sukumaran, K., McConnell, R., Berhane, K., Schwartz, J., Hackman, D.A., Ahmadi, H., Chen, J.-C., Herting, M.M., 2023. Effects of ambient fine particulates, nitrogen dioxide, and ozone on maturation of functional brain networks across early adolescence. *Environ. Int.* 177, 108001. <https://doi.org/10.1016/j.envint.2023.108001>.

Cserbik, D., Chen, J.-C., McConnell, R., Berhane, K., Sowell, E.R., Schwartz, J., Hackman, D.A., Kan, E., Fan, C.C., Herting, M.M., 2020. Fine particulate matter exposure during childhood relates to hemispheric-specific differences in brain structure. *Environ. Int.* 143, 105933. <https://doi.org/10.1016/j.envint.2020.105933>.

Darby, S., Hill, D., Auvinen, A., Barros-Dios, J.M., Baysson, H., Bochicchio, F., Deo, H., Falk, R., Forastiere, F., Hakama, M., Heid, I., Kreienbrock, L., Kreuzer, M., Lagarde, F., Mäkeläinen, I., Muirhead, C., Oberaigner, W., Pershagen, G., Ruano-Ravina, A., Doll, R., 2005. Radon in homes and risk of lung cancer: collaborative analysis of individual data from 13 European case-control studies. *BMJ (Clin. Res. Ed.)* 330 (7485), 223. <https://doi.org/10.1136/bmj.38308.477650.63>.

Di Dona, G., Ronconi, L., 2023. Beta oscillations in vision: a (preconscious) neural mechanism for the dorsal visual stream? *Front. Psychol.* 14. <https://doi.org/10.3389/fpsyg.2023.1296483>.

Dong, H.-M., Zhang, X.-H., Labache, L., Zhang, S., Ooi, L.Q.R., Yeo, B.T.T., Margulies, D.S., Holmes, A.J., Zuo, X.-N., 2024. Ventral attention network connectivity is linked to cortical maturation and cognitive ability in childhood. *Nat. Neurosci.* 27 (10), 2009–2020. <https://doi.org/10.1038/s41593-024-01736-x>.

Du Rietz, E., Cheung, C.H.M., McLoughlin, G., Brandeis, D., Banaschewski, T., Asherson, P., Kuntsi, J., 2016. Self-report of ADHD shows limited agreement with objective markers of persistence and remittance. *J. Psychiatr. Res.* 82, 91–99. <https://doi.org/10.1016/j.jpsychires.2016.07.020>.

Efron, B., Tibshirani, R., 1986. Bootstrap methods for standard errors, confidence intervals, and other measures of statistical accuracy. *Stat. Sci.* 1 (1), 54–75. <https://doi.org/10.1214/ss/1177013815>.

Engel, A.K., Fries, P., 2010. Beta-band oscillations—signalling the status quo? *Curr. Opin. Neurobiol.* 20 (2), 156–165. <https://doi.org/10.1016/j.conb.2010.02.015>.

Ernst, M.D., 2004. Permutation methods: a basis for exact inference. *Stat. Sci.* 19 (4), 676–685. <https://doi.org/10.1214/088342304000000396>.

- Farrant, K., Uddin, L.Q., 2015. Asymmetric development of dorsal and ventral attention networks in the human brain. *Dev. Cogn. Neurosci.* 12, 165–174. <https://doi.org/10.1016/j.dcn.2015.02.001>.
- Franceschini, S., Bertoni, S., Puccio, G., Gori, S., Termine, C., Facoetti, A., 2022. Visuospatial attention deficit in children with reading difficulties. *Sci. Rep.* 12 (1), 13930. <https://doi.org/10.1038/s41598-022-16646-w>.
- Fritz, M.S., MacKinnon, D.P., 2007. Required sample size to detect the mediated effect. *Psychol. Sci.* 18 (3), 233–239. <https://doi.org/10.1111/j.1467-9280.2007.01882.x>.
- Fung, M.H., Taylor, B.K., Frenzel, M.R., Eastman, J.A., Wang, Y.-P., Calhoun, V.D., Stephen, J.M., Wilson, T.W., 2020. Pubertal testosterone tracks the developmental trajectory of neural oscillatory activity serving visuospatial processing. *Cereb. Cortex* 30 (11), 5960–5971. <https://doi.org/10.1093/cercor/bhaa169>.
- Fung, M.H., Rahman, R.L., Taylor, B.K., Frenzel, M.R., Eastman, J.A., Wang, Y.-P., Calhoun, V.D., Stephen, J.M., Wilson, T.W., 2022. The impact of pubertal DHEA on the development of visuospatial oscillatory dynamics. *Hum. Brain Mapp.* 43 (17), 5154–5166. <https://doi.org/10.1002/hbm.25991>.
- Geng, J.J., Vossel, S., 2013. Re-evaluating the role of TPJ in attentional control: contextual updating? *Neurosci. Biobehav. Rev.* 37 (10, Part 2), 2608–2620. <https://doi.org/10.1016/j.neubiorev.2013.08.010>.
- Gola, M., Magnuski, M., Szumska, I., Wróbel, A., 2013. EEG beta band activity is related to attention and attentional deficits in the visual performance of elderly subjects. *Int. J. Psychophysiol.* 89 (3), 334–341. <https://doi.org/10.1016/j.ijpsycho.2013.05.007>.
- Goldman, L.R., 1995. Children—unique and vulnerable. Environmental risks facing children and recommendations for response. *Environ. Health Perspect.* 103 (6), 13–18. <https://doi.org/10.1289/ehp.95103s613>.
- Gómez-Anca, S., Barros-Dios, J.M., 2020. Radon exposure and neurodegenerative disease. *Article 20. Int. J. Environ. Res. Public Health* 17 (20). <https://doi.org/10.3390/ijerph17207439>.
- Gross, J., Kujala, J., Hämäläinen, M., Timmermann, L., Schnitzler, A., Salmelin, R., 2001. Dynamic imaging of coherent sources: studying neural interactions in the human brain. *Proc. Natl. Acad. Sci.* 98 (2), 694–699. <https://doi.org/10.1073/pnas.98.2.694>.
- Gross, J., Baillet, S., Barnes, G.R., Henson, R.N., Hillebrand, A., Jensen, O., Jerbi, K., Litvak, V., Maess, B., Oostenveld, R., Parkkonen, L., Taylor, J.R., van Wassenhove, V., Wibral, M., Schoffelen, J.-M., 2013. Good practice for conducting and reporting MEG research. *NeuroImage* 65, 349–363. <https://doi.org/10.1016/j.neuroimage.2012.10.001>.
- Grzywa-Celińska, A., Krusiński, A., Mazur, J., Szewczyk, K., Kozak, K., 2020. Radon—the element of risk. The impact of radon exposure on human health. *Toxics* 8 (4), 120. <https://doi.org/10.3390/toxics8040120>.
- Güntekin, B., Emek-Savaş, D.D., Kurt, P., Yener, G.G., Başar, E., 2013. Beta oscillatory responses in healthy subjects and subjects with mild cognitive impairment. *NeuroImage Clin.* 3, 39–46. <https://doi.org/10.1016/j.nicl.2013.07.003>.
- Guo, D., Zhan, C., Liu, J., Wang, Z., Cui, M., Zhang, X., Su, X., Pan, L., Deng, M., Zhao, L., Liu, J., Song, Y., 2022. Alternations in neural oscillation related to attention network reveal influence of indoor toluene on cognition at low concentration. *Indoor Air* 32 (7), e13067. <https://doi.org/10.1111/ina.13067>.
- Guo, T., Najafi, M.L., Zhang, J., 2025. A systematic review of exposure to toxic elements and neurocognitive development in children. *Ecotoxicol. Environ. Saf.* 291, 117792. <https://doi.org/10.1016/j.ecoenv.2025.117792>.
- Herting, M.M., Bottenhorn, K.L., Cotter, D.L., 2024. Outdoor air pollution and brain development in childhood and adolescence. *Trends Neurosci.* 47 (8), 593–607. <https://doi.org/10.1016/j.tins.2024.06.008>.
- Hillebrand, A., Singh, K.D., Holliday, I.E., Furlong, P.L., Barnes, G.R., 2005. A new approach to neuroimaging with magnetoencephalography. *Hum. Brain Mapp.* 25 (2), 199–211. <https://doi.org/10.1002/hbm.20102>.
- Jiang, B., Ding, L., Chen, K., Huang, Q., Han, X., Jin, Z., Cao, L.-Z., Zhang, J., Li, Q., Xue, C., He, Y., Fang, B., Pei, G., Yan, T., 2024. Beta oscillation modulations of the orienting attention network effect correlate with dopamine-dependent motor symptoms of Parkinson's disease. *Brain Struct. Funct.* 230 (1), 4. <https://doi.org/10.1007/s00429-024-02863-8>.
- Junghöfer, M., Elbert, T., Tucker, D.M., Rockstroh, B., 2000. Statistical control of artifacts in dense array EEG/MEG studies. *Psychophysiology* 37 (4), 523–532. <https://doi.org/10.1111/1469-8986.3740523>.
- Kang, J.-K., Seo, S., Jin, Y.W., 2019. Health effects of radon exposure. *Yonsei Med. J.* 60 (7), 597–603. <https://doi.org/10.3349/ymj.2019.60.7.597>.
- Killanin, A.D., Wiesman, A.I., Heinrichs-Graham, E., Groff, B.R., Frenzel, M.R., Eastman, J.A., Wang, Y.-P., Calhoun, V.D., Stephen, J.M., Wilson, T.W., 2020. Development and sex modulate visuospatial oscillatory dynamics in typically-developing children and adolescents. *NeuroImage* 221, 117192. <https://doi.org/10.1016/j.neuroimage.2020.117192>.
- Konrad, K., Neufang, S., Thiel, C.M., Specht, K., Hanisch, C., Fan, J., Herpertz-Dahlmann, B., Fink, G.R., 2005. Development of attentional networks: an fMRI study with children and adults. *NeuroImage* 28 (2), 429–439. <https://doi.org/10.1016/j.neuroimage.2005.06.065>.
- Kusters, M.S.W., Granés, L., Petricola, S., Tiemeier, H., Muetzel, R.L., Guxens, M., 2025. Exposure to residential air pollution and the development of functional connectivity of brain networks throughout adolescence. *Environ. Int.* 196, 109245. <https://doi.org/10.1016/j.envint.2024.109245>.
- Larsen, B., Luna, B., 2018. Adolescence as a neurobiological critical period for the development of higher-order cognition. *Neurosci. Biobehav. Rev.* 94, 179–195. <https://doi.org/10.1016/j.neubiorev.2018.09.005>.
- Li, X., Motwani, C., Cao, M., Martin, E., Halperin, J.M., 2023. Working memory-related neurofunctional correlates associated with the frontal lobe in children with familial vs. non-familial attention deficit/hyperactivity disorder. *Brain Sci.* 13 (10), 1469. <https://doi.org/10.3390/brainsci13101469>.
- Long, J.A., 2019. *Interact. Compr. Use Friendly Toolkit Probing Interact.*
- Long, J.A., 2022. *jtools Anal. Present. Soc. Sci. Data.*
- Maris, E., Oostenveld, R., 2007. Nonparametric statistical testing of EEG- and MEG-data. *J. Neurosci. Methods* 164 (1), 177–190. <https://doi.org/10.1016/j.jneumeth.2007.03.024>.
- Miller, J.G., Gillette, J.S., Manczak, E.M., Kircanski, K., Gotlib, I.H., 2019. Fine particle air pollution and physiological reactivity to social stress in adolescence: the moderating role of anxiety and depression. *Biopsychosoc. Sci. Med.* 81 (7), 641. <https://doi.org/10.1097/PSY.0000000000000714>.
- Min, J., Min, K., 2017. Exposure to ambient PM10 and NO2 and the incidence of attention-deficit hyperactivity disorder in childhood. *Environ. Int.* 99, 221–227. <https://doi.org/10.1016/j.envint.2016.11.022>.
- Myhre, O., Låg, M., Villanger, G.D., Ofteidal, B., Øvrevik, J., Holme, J.A., Aase, H., Paulsen, R.E., Bal-Price, A., Dirven, H., 2018. Early life exposure to air pollution particulate matter (PM) as risk factor for attention deficit/hyperactivity disorder (ADHD): need for novel strategies for mechanisms and causalities. *Toxicol. Appl. Pharmacol.* 354, 196–214. <https://doi.org/10.1016/j.taap.2018.03.015>.
- Neubauer, A.C., Fink, A., 2009. Intelligence and neural efficiency: measures of brain activation versus measures of functional connectivity in the brain. *Intelligence* 37 (2), 223–229. <https://doi.org/10.1016/j.intell.2008.10.008>.
- Newman, N.C., Ryan, P., LeMasters, G., Levin, L., Bernstein, D., Hershey, G.K.K., Lockey, J.E., Villareal, M., Reponen, T., Grinshpun, S., Sucharew, H., Dietrich, K.N., 2013. Traffic-related air pollution exposure in the first year of life and behavioral scores at 7 years of age. *Environ. Health Perspect.* 121 (6), 731–736. <https://doi.org/10.1289/ehp.1205555>.
- Nickel, K., Tebartz van Elst, L., Manko, J., Unterrainer, J., Rauh, R., Klein, C., Endres, D., Kaller, C.P., Mader, I., Riedel, A., Biscaldi, M., Maier, S., 2018. Inferior frontal gyrus volume loss distinguishes between autism and (comorbid) attention-deficit/hyperactivity disorder—a freesurfer analysis in children. *Front. Psychiatry* 9. <https://doi.org/10.3389/fpsy.2018.00521>.
- Novilla, M.L.B., Johnston, J.D., Beard, J.D., Pettit, L.L., Davis, S.F., Johnson, C.E., 2021. Radon awareness and policy perspectives on testing and mitigation. *Article 8. Atmosphere* 12 (8). <https://doi.org/10.3390/atmos12081016>.
- Perera, F., Viswanathan, S., Whyatt, R., Tang, D., Miller, R.L., Rauh, V., 2006. Children's environmental health research—highlights from the columbia center for children's environmental health. *Ann. N. Y. Acad. Sci.* 1076 (1), 15–28. <https://doi.org/10.1196/annals.1371.018>.
- Peterson, B.S., Rauh, V.A., Bansal, R., Hao, X., Toth, Z., Nati, G., Walsh, K., Miller, R.L., Arias, F., Semanek, D., Perera, F., 2015. Effects of prenatal exposure to air pollutants (polycyclic aromatic hydrocarbons) on the development of brain white matter, cognition, and behavior in later childhood. *JAMA Psychiatry* 72 (6), 531. <https://doi.org/10.1001/jamapsychiatry.2015.57>.
- Picci, G., Ott, L.R., Petro, N.M., Casagrande, C.C., Killanin, A.D., Rice, D.L., Coutant, A.T., Arif, Y., Embury, C.M., Okelberry, H.J., Johnson, H.J., Springer, S.D., Pulliam, H.R., Wang, Y.-P., Calhoun, V.D., Stephen, J.M., Heinrichs-Graham, E., Taylor, B.K., Wilson, T.W., 2023. Developmental alterations in the neural oscillatory dynamics underlying attentional reorienting. *Dev. Cogn. Neurosci.* 63, 101288. <https://doi.org/10.1016/j.dcn.2023.101288>.
- Pisella, L., Vialatte, A., Martel, M., Prost-Lefebvre, M., Caton, M.-C., Stalder, M., Yssad, R., Roy, A.C., Vuillerot, C., Gonzalez-Monge, S., 2021. Elementary visuospatial perception deficit in children with neurodevelopmental disorders. *Dev. Med. Child Neurol.* 63 (4), 457–464. <https://doi.org/10.1111/dmcn.14743>.
- Pulliam, H.R., Springer, S.D., Rice, D.L., Ende, G.C., Johnson, H.J., Willett, M.P., Wilson, T.W., Taylor, B.K., 2024. Neurotoxic effects of home radon exposure on oscillatory dynamics serving attentional orienting in children and adolescents. *NeuroImage* 292, 120606. <https://doi.org/10.1016/j.neuroimage.2024.120606>.
- Rauh, V.A., Margolis, A.E., 2016. Research review: environmental exposures, neurodevelopment, and child mental health – new paradigms for the study of brain and behavioral effects. *J. Child Psychol. Psychiatry* 57 (7), 775–793. <https://doi.org/10.1111/jcpp.12537>.
- Reynolds, C.R., Kamphaus, R.W., 2015. *Behavior assessment for children, 3rd ed.* NCS Pearson, Inc. (BASC-3), Bloomington.
- Riudavets, M., Garcia de Herrerros, M., Besse, B., Mezquita, L., 2022. Radon and lung cancer: current trends and future perspectives. *Cancers* 14 (13), 3142. <https://doi.org/10.3390/cancers14133142>.
- Roberts, S., Arseneault, L., Barratt, B., Beevers, S., Danese, A., Odgers, C.L., Moffitt, T.E., Reuben, A., Kelly, F.J., Fisher, H.L., 2019. Exploration of NO2 and PM2.5 air pollution and mental health problems using high-resolution data in London-based children from a UK longitudinal cohort study. *Psychiatry Res.* 272, 8–17. <https://doi.org/10.1016/j.psychres.2018.12.050>.
- Samea, F., Soluki, S., Nejati, V., Zarei, M., Cortese, S., Eickhoff, S.B., Tahmasian, M., Eickhoff, C.R., 2019. Brain alterations in children/adolescents with ADHD revisited: a neuroimaging meta-analysis of 96 structural and functional studies. *Neurosci. Biobehav. Rev.* 100, 1–8. <https://doi.org/10.1016/j.neubiorev.2019.02.011>.
- Schul, R., Townsend, J., Stiles, J., 2003. The development of attentional orienting during the school-age years. *Dev. Sci.* 6 (3), 262–272. <https://doi.org/10.1111/1467-7687.00282>.
- Sethi, T.K., El-Ghamry, M.N., Kloecker, G.H., 2012. Radon and lung cancer. *Clin. Adv. Hematol. Oncol. HO* 10 (3), 157–164.
- Slobodina, O., Davidovitch, M., 2022. Primary school children's self-reports of attention deficit hyperactivity disorder-related symptoms and their associations with subjective and objective measures of attention deficit hyperactivity disorder. *Front. Hum. Neurosci.* 16. <https://doi.org/10.3389/fnhum.2022.806047>.
- Smith, O.V., Penhale, S.H., Ott, L.R., Rice, D.L., Coutant, A.T., Glesinger, R., Wilson, T.W., Taylor, B.K., 2024. Everyday home radon exposure is associated with altered

- structural brain morphology in youths. *Neurotoxicology* 102, 114–120. <https://doi.org/10.1016/j.neuro.2024.04.007>.
- Solis-Vivanco, R., Jensen, O., Bonnefond, M., 2021. New insights on the ventral attention network: active suppression and involuntary recruitment during a bimodal task. *Hum. Brain Mapp.* 42 (6), 1699–1713. <https://doi.org/10.1002/hbm.25322>.
- Swick, D., Ashley, V., Turken, A.U., 2008. Left inferior frontal gyrus is critical for response inhibition. *BMC Neurosci.* 9 (1), 102. <https://doi.org/10.1186/1471-2202-9-102>.
- Taulu, S., Simola, J., 2006. Spatiotemporal signal space separation method for rejecting nearby interference in MEG measurements. *Phys. Med. Biol.* 51 (7), 1759–1768. <https://doi.org/10.1088/0031-9155/51/7/008>.
- Taulu, S., Simola, J., Kajola, M., 2005. Applications of the signal space separation method. *IEEE Trans. Signal Process.* 53 (9), 3359–3372. <https://doi.org/10.1109/TSP.2005.853302>.
- Taylor, B.K., Eastman, J.A., Frenzel, M.R., Embury, C.M., Wang, Y.-P., Calhoun, V.D., Stephen, J.M., Wilson, T.W., 2021. Neural oscillations underlying selective attention follow sexually divergent developmental trajectories during adolescence. *Dev. Cogn. Neurosci.* 49, 100961. <https://doi.org/10.1016/j.dcn.2021.100961>.
- Taylor, B.K., Heinrichs-Graham, E., Eastman, J.A., Frenzel, M.R., Wang, Y.-P., Calhoun, V.D., Stephen, J.M., Wilson, T.W., 2022. Longitudinal changes in the neural oscillatory dynamics underlying abstract reasoning in children and adolescents. *NeuroImage* 253, 119094. <https://doi.org/10.1016/j.neuroimage.2022.119094>.
- Taylor, B.K., Smith, O.V., Miller, G.E., 2022. Chronic home radon exposure is associated with higher inflammatory biomarker concentrations in children and adolescents. *Int. J. Environ. Res. Public Health* 20 (1), 246. <https://doi.org/10.3390/ijerph20010246>.
- Taylor, B.K., Pulliam, H., Smith, O.V., Rice, D.L., Johnson, H.J., Coutant, A.T., Glesinger, R., Wilson, T.W., 2024. Effects of chronic home radon exposure on cognitive, behavioral, and mental health in developing children and adolescents. *Front. Psychol.* 15, 1330469. <https://doi.org/10.3389/fpsyg.2024.1330469>.
- Taylor, B.K., Bonney, R.A., Thompson, D., Greenwood, S.L., Clarke-Smith, M.N., Rasmussen, S.C., Parolek, G.E., Smith, O.V., Pulliam, H.R., Miller, G.E., 2025. Inflammation-related aberrations in beta and gamma oscillatory dynamics serving attention processing in typically-developing youth. *Brain Commun.*, fcfa485 <https://doi.org/10.1093/braincomms/fcfa485>.
- Thapar, A., Cooper, M., Eyre, O., Langley, K., 2013. Practitioner review: what have we learnt about the causes of ADHD? *J. Child Psychol. Psychiatry* 54 (1), 3–16. <https://doi.org/10.1111/j.1469-7610.2012.02611.x>.
- Thygesen, M., Holst, G.J., Hansen, B., Geels, C., Kalkbrenner, A., Schendel, D., Brandt, J., Pedersen, C.B., Dalgaard, S., 2020. Exposure to air pollution in early childhood and the association with attention-deficit hyperactivity disorder. *Environ. Res.* 183, 108930. <https://doi.org/10.1016/j.envres.2019.108930>.
- Tosoni, A., Capotosto, P., Baldassarre, A., Spadone, S., Sestieri, C., 2023. Neuroimaging evidence supporting a dual-network architecture for the control of visuospatial attention in the human brain: a mini review. *Front. Hum. Neurosci.* 17, 1250096. <https://doi.org/10.3389/fnhum.2023.1250096>.
- Trés, E.S., Brucki, S.M.D., 2014. Visuospatial processing: a review from basic to current concepts. *Dement. Neuropsychol.* 8 (2), 175–181. <https://doi.org/10.1590/S1980-57642014DN82000014>.
- Uhlhaas, P.J., Roux, F., Singer, W., Haenschel, C., Sireteanu, R., Rodriguez, E., 2009. The development of neural synchrony reflects late maturation and restructuring of functional networks in humans. *Proc. Natl. Acad. Sci.* 106 (24), 9866–9871. <https://doi.org/10.1073/pnas.0900390106>.
- United States Environmental Protection Agency, 2016. A citizen's guide to radon: the guide to protecting yourself and your family from radon (EP 402/K-12/002). Indoor Environments Division (6609J), Washington DC.
- Uusitalo, M.A., Ilmoniemi, R.J., 1997. Signal-space projection method for separating MEG or EEG into components. *Med. Biol. Eng. Comput.* 35 (2), 135–140. <https://doi.org/10.1007/BF02534144>.
- Van Ewijk, H., Weeda, W.D., Heslenfeld, D.J., Luman, M., Hartman, C.A., Hoekstra, P.J., Faraone, S.V., Franke, B., Buitelaar, J.K., Oosterlaan, J., 2015. Neural correlates of visuospatial working memory in attention-deficit/hyperactivity disorder and healthy controls. *Psychiatry Res. Neuroimaging* 233 (2), 233–242. <https://doi.org/10.1016/j.pscychres.2015.07.003>.
- Van Veen, B.D., van Drongelen, W., Yuchtman, M., Suzuki, A., 1997. Localization of brain electrical activity via linearly constrained minimum variance spatial filtering. *IEEE Trans. BioMed. Eng.* 44 (9), 867–880. <https://doi.org/10.1109/10.623056>.
- Vincent, A., 1992. Methods for improving the signal-to-noise ratio of endogenous-evoked potentials. *Integr. Physiol. Behav. Sci.* 27 (1), 54–65. <https://doi.org/10.1007/BF02691092>.
- Vogeltanz-Holm, N., Schwartz, G.G., 2018. Radon and lung cancer: what does the public really know? *J. Environ. Radioact.* 192, 26–31. <https://doi.org/10.1016/j.jenvrad.2018.05.017>.
- Vossel, S., Geng, J.J., Fink, G.R., 2014. Dorsal and ventral attention systems: distinct neural circuits but collaborative roles. *Neuroscientist* 20 (2), 150–159. <https://doi.org/10.1177/1073858413494269>.
- Wang, S., Yang, Y., Xing, W., Chen, J., Liu, C., Luo, X., 2013. Altered neural circuits related to sustained attention and executive control in children with ADHD: an event-related fMRI study. *Clin. Neurophysiol.* 124 (11), 2181–2190. <https://doi.org/10.1016/j.clinph.2013.05.008>.
- Wiesman, A.I., Heinrichs-Graham, E., Proskovec, A.L., McDermott, T.J., Wilson, T.W., 2017. Oscillations during observations: dynamic oscillatory networks serving visuospatial attention. *Hum. Brain Mapp.* 38 (10), 5128–5140. <https://doi.org/10.1002/hbm.23720>.
- Wróbel, A., 2000. Beta activity: a carrier for visual attention. *Article 2 Acta Neurobiol. Exp.* 60 (2). <https://doi.org/10.55782/ane-2000-1344>.
- Wylie, A.C., Short, S.J., 2023. Environmental toxicants and the developing brain. *Biol. Psychiatry* 93 (10), 921–933. <https://doi.org/10.1016/j.biopsych.2023.01.007>.
- Zhang, Y., Lu, L., Chen, C., Field, R.W., D'Alton, M., Kahe, K., 2022. Does protracted radon exposure play a role in the development of dementia? *Environ. Res.* 210, 112980. <https://doi.org/10.1016/j.envres.2022.112980>.